Insights into ErbB signaling from the structure of the ErbB2-pertuzumab complex

Matthew C. Franklin,[1,5] Kendall D. Carey,[2,5] Felix F. Vajdos,[1,6] Daniel J. Leahy,[3,4] Abraham M. de Vos,[1,*] and Mark X. Sliwkowski[2,*]

[1]Department of Protein Engineering
[2]Department of Molecular Oncology
Genentech, Inc., 1 DNA Way, South San Francisco, California 94114
[3]Department of Biophysics and Biophysical Chemistry
[4]Howard Hughes Medical Institute
The Johns Hopkins University School of Medicine, 725 North Wolfe Street, Baltimore, Maryland 21205
[5]These authors contributed equally to this work.
[6]Present address: Pfizer, Inc., Eastern Point Road, Groton, Connecticut 06340
*Correspondence: devos@gene.com (A.M.dV.); marks@gene.com (M.X.S.)

Summary

We have determined the 3.2 Å X-ray crystal structure of the extracellular domain of the human epidermal growth factor receptor 2 (ErbB2 or HER2) in a complex with the antigen binding fragment of pertuzumab, an anti-ErbB2 monoclonal antibody also known as 2C4 or Omnitarg. Pertuzumab binds to ErbB2 near the center of domain II, sterically blocking a binding pocket necessary for receptor dimerization and signaling. The ErbB2-pertuzumab structure, combined with earlier mutagenesis data, defines the pertuzumab residues essential for ErbB2 interaction. To analyze the ErbB2 side of the interface, we have mutated a number of residues contacting pertuzumab and examined the effects of these mutations on pertuzumab binding and ErbB2-ErbB3 heterodimerization. We have also shown that conserved residues previously shown to be necessary for EGF receptor homodimerization may be dispensible for ErbB2-ErbB3 heterodimerization.

Introduction

Epidermal growth factor receptors (also known as ErbBs) and their ligands exist in all higher eukaryotes, including *C. elegans* (Aroian et al., 1990) and *Drosophila* (Livneh et al., 1985; Wadsworth et al., 1985), and have been implicated in a number of cancers due to dysregulation or mutation of the ErbB genes (Burgess et al., 2003; Holbro et al., 2003; Yarden and Sliwkowski, 2001). The mammalian ErbB system contains four receptors, 40%–45% identical to one another, which arose from a series of gene duplications early in vertebrate evolution (Stein and Staros, 2000). The ErbBs have a common architecture, details of which have been revealed recently by a series of structures of the extracellular domains of EGF receptor (EGFR or ErbB1) (Ferguson et al., 2003; Garrett et al., 2002; Ogiso et al., 2002), ErbB2 (HER2) (Cho et al., 2003; Garrett et al., 2003), and ErbB3 (HER3) (Cho and Leahy, 2002), as well as the intracellular kinase domain of EGFR (Stamos et al., 2002). The ErbBs are type 1 transmembrane proteins, with a ligand binding extracellular portion containing four domains (I, II, III, and IV), a single transmembrane helix, a tyrosine kinase domain most closely related to the Janus kinases and in the same family as other receptor tyrosine kinases (Hanks and Hunter, 1995), and a C-terminal tail (the length of which varies between family members) containing a number of tyrosine phosphorylation sites that serve as a scaffold for adaptor molecules and enzymes to facilitate downstream signaling (Jorissen et al., 2003; Schlessinger, 2000).

At least twelve ligands are known to bind mammalian ErbBs, including epidermal growth factor (EGF) and neuregulins (or heregulins) (Falls, 2003). A comparison of structures of ErbB3 and EGF receptor monomers versus a ligand-bound EGFR dimer shows that the ligand binds at a site between domains I and III and induces (or at least stabilizes) a dramatic conformational change in the receptor extracellular domain (Cho and Leahy, 2002; Ferguson et al., 2003; Garrett et al., 2002; Ogiso et al., 2002). ErbB2 is the only ErbB for which no ligand has been found; the structure of the ErbB2 extracellular domain shows that the ligand binding site has closed up so that domains I and III contact each other directly (Cho et al., 2003; Garrett et al.,

SIGNIFICANCE

ErbB2 is overexpressed in a number of types of cancer, particularly breast cancer, where overexpression correlates strongly with a more aggressive disease and poorer survival rates. The anti-ErbB2 monoclonal antibody trastuzumab (Herceptin) is indicated for patients whose metastatic tumors overexpress ErbB2. In contrast, pertuzumab (Omnitarg) is currently being evaluated in Phase II clinical trials in patients whose breast, non-small cell lung, prostate, or ovarian tumors do not contain the amplified ErbB2 gene. Our ErbB2-pertuzumab structure clearly shows how pertuzumab inhibits ErbB2's function as a coreceptor in ligand-mediated ErbB signaling, and provides a framework for interpretation of previous pertuzumab mutagenesis data.

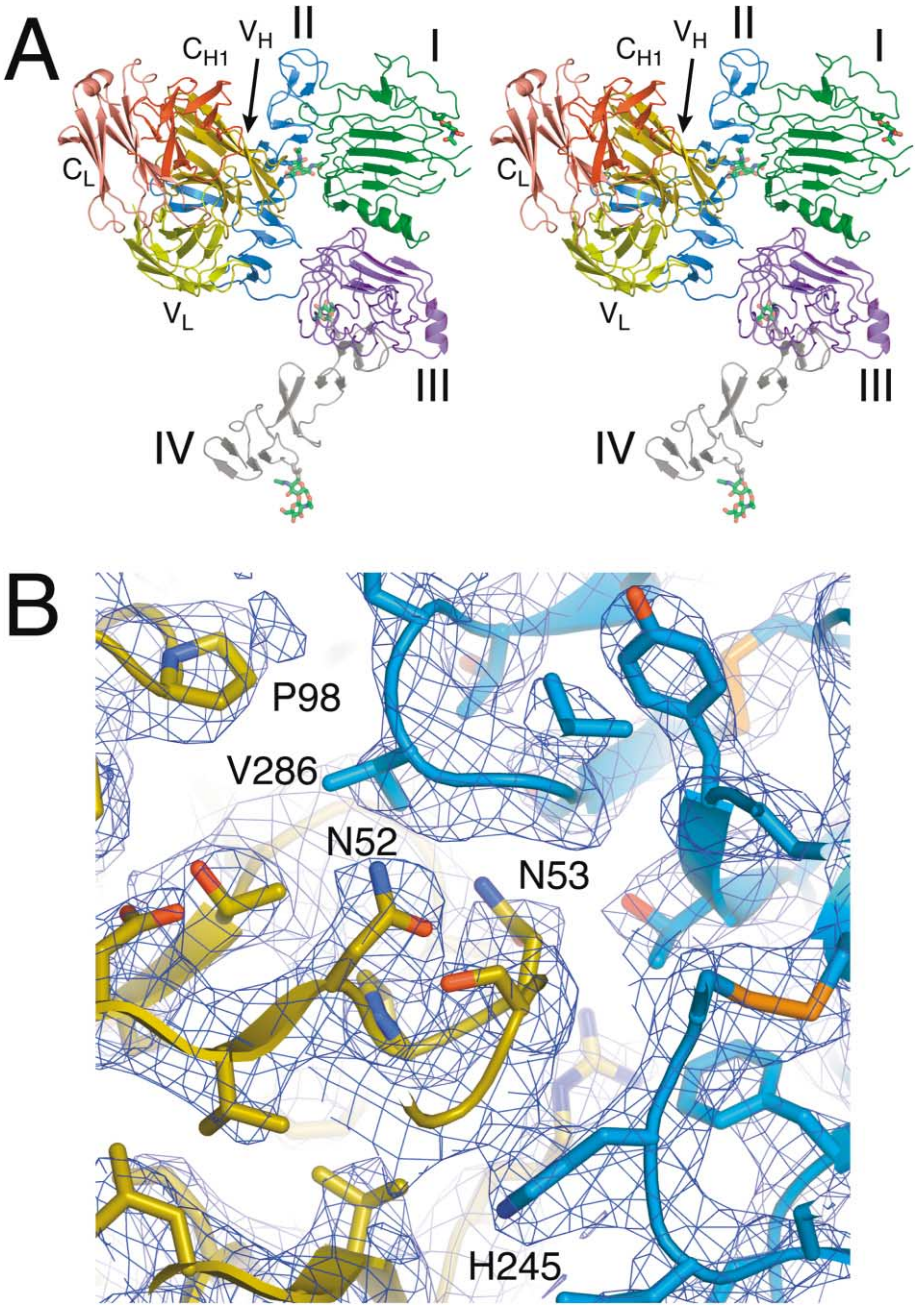

Figure 1. The ErbB2-pertuzumab complex

A: A ribbon representation of chains B, E, and F from the ErbB2-pertuzumab complex is shown in stereo. ErbB2 is colored by domain, with domain I (residues 1–195) in green, domain II (196–320) in blue, domain III (321–488) in purple, and domain IV (489–560) in gray. Pertuzumab is colored by domain and chain, with the light chain variable domain (residues 1–109) in light yellow, heavy chain variable domain (1–113) in gold, light chain constant domain (110–214) in pink, and heavy chain constant domain (114–216) in red. Glycosylation on ErbB2 is shown in stick form, with carbons colored green, nitrogens blue, and oxygens red.

B: A composite-omit electron density map of a portion of the ErbB2-pertuzumab interface, contoured at 1.3 sigma, is shown as a blue mesh. The refined ErbB2-pertuzumab model is superimposed, with side chains in stick form and backbone in ribbon form. Carbons are colored by domain as in **A**: ErbB2 domain II in blue, and pertuzumab V_H in gold.

2003). The residues comprising the former binding site are not conserved relative to the rest of the ErbB family (Garrett et al., 2003), suggesting that ErbB2 is no longer capable of binding a ligand.

Ligand-induced dimerization provides the normal downstream signaling mechanism for the ErbBs (Burgess et al., 2003). A possible structural mechanism for dimerization is suggested by the ligand-induced conformational change. When unliganded, the extracellular domain of EGFR and ErbB3 (and presumably ErbB4) is in a "closed" conformation, with a β hairpin in domain II interacting with a portion of domain IV (Cho and Leahy, 2002; Ferguson et al., 2003). In the ligand-bound, "open" state, the domain II hairpin now protrudes out from the rest of the molecule, and makes most of the contacts seen in the EGF receptor dimer (Garrett et al., 2002; Ogiso et al., 2002). It should be noted that the open conformation of EGFR has not yet been observed except in the context of an EGFR homodimer. The ErbB2 extracellular domain is always in the open conformation, even when monomeric (Cho et al., 2003; Garrett et al., 2003), which may explain why it is the preferred dimerization partner for the other three family members (Graus-Porta et al., 1997). By mechanisms that are still unclear structurally, dimerization brings the intracellular kinase domains of the two ErbBs into proximity, allowing transphosphorylation of tyrosines on the C-terminal tail of one ErbB by the kinase domain of the other (Jorissen et al., 2003), and the consequent recruitment of various

enzymes and adaptor molecules for further downstream signaling (Olayioye et al., 2000).

ErbB2 overexpression in breast cancer correlates well with increased tumor growth rates, higher metastatic potential, and poorer long-term survival rates for the patient (Holbro et al., 2003; Paik and Liu, 2000; Ross and Fletcher, 1998; Slamon et al., 1987). A number of therapeutic approaches are being developed to block the effects of ErbB2 overexpression (Arteaga, 2003; Fry, 2003), including the humanized monoclonal antibodies trastuzumab (Carter et al., 2000) and pertuzumab (2C4 or Omnitarg). Trastuzumab is approved for metastatic breast cancer patients whose tumors overexpress ErbB2 (Cobleigh et al., 1999; Slamon et al., 2001; Vogel et al., 2002), while pertuzumab is currently in phase II clinical trials. Trastuzumab and pertuzumab bind to different epitopes in the the extracellular domain of ErbB2, as has been seen functionally (Fendly et al., 1990) and structurally (Cho et al., 2003, and this work). Pertuzumab binding mediates the same antibody-dependent cytotoxic effects as trastuzumab binding (Clynes et al., 2000) (K. Totpal, personal communication), although it does not block ErbB2 shedding as trastuzumab does (Molina et al., 2001). In addition to cytotoxic effects, pertuzumab binding directly inhibits ErbB2 association with its partner receptors, blocking the signaling cascade at its source (Agus et al., 2002). In experimental systems where ErbB2 is activated but not overexpressed, the Fab fragment of pertuzumab, which will not cause antibody-dependent cytotoxicity, appears to be just as effective as the intact MAb at inhibiting ErbB2-mediated signaling, in contrast to the ineffectiveness of the trastuzumab Fab (Agus et al., 2002; Kelley et al., 1992). This property may explain why pertuzumab, unlike trastuzumab, is effective against a broad range of cancers which do not express ErbB2 at high levels (Agus et al., 2000, 2002; Mann et al., 2001; Mendoza et al., 2002).

To more fully understand the mechanism of action of pertuzumab, we have determined the cocrystal structure of the pertuzumab Fab bound to the extracellular domain of ErbB2. This structure represents the pharmacologically relevant complex, given the efficacy of the pertuzumab Fab in vitro and in vivo (Agus et al., 2002). Previous structural and mutagenic analysis of pertuzumab (Vajdos et al., 2002) can now be reinterpreted to provide an understanding of pertuzumab binding from one side of the interface. To analyze the other side of the interface, we have mutated a number of ErbB2 residues in and around the pertuzumab binding site, and examined the effects of these mutations on pertuzumab binding, as well as ErbB2-ErbB3 heterodimerization. Finally, the overlap between the pertuzumab binding site on ErbB2 and the probable heterodimer interface suggests that the binding of the antibody sterically interferes with ErbB2 dimerization and signaling.

Results

ErbB2-pertuzumab structure

The soluble extracellular domain of ErbB2 (Hudziak and Ullrich, 1991) was crystallized in complex with the Fab fragment of the anti-ErbB2 monoclonal antibody pertuzumab (2C4) (Vajdos et al., 2002). The structure of this complex was solved to 3.25 Å by molecular replacement with the program AMoRe (Navaza, 1994), using the structure of rat ErbB2 extracellular domain (Cho et al., 2003) as a search model. There are two ErbB2-pertuzumab complexes in the asymmetric unit of this crystal, related by a noncrystallographic 2-fold axis next to residue 162 in domain I; this domain I-domain I interaction buries only 500 Å^2 per monomer and is probably not biologically relevant. One complex (chains B, E, and F) is slightly better ordered than the other, and is shown in Figure 1A. After finding both copies of ErbB2 by molecular replacement, it was possible to locate the variable domains of the two pertuzumab Fabs in a subsequent molecular replacement search, then finally place the constant domain of the Fabs. The structure has been refined to an R factor of 22.4% (free R 26.8%), with acceptable model geometry (Table 1). While peripheral portions of the structure are not well ordered (see below), the interface between ErbB2 and pertuzumab has clear electron density (Figure 1B).

Table 1. Data collection and refinement statistics

Data collection statistics	ErbB2-pertuzumab complex	
Space group	$P4_3\,2_1\,2$	
Unit cell (Å)	139.4, 139.4, 356.9	
Beamline, wavelength	ALS 5.0.2, 1.00 Å	
Unique reflections	56351	
Resolution (Å)	30.0–3.25	3.37–3.25
R_{sym}	0.116	0.691
Completeness (%)	99.9	100.0
Avg. redundancy	8.2	8.3
$I/\sigma(I)$	19.3	3.3
Refinement statistics		
Resolution (Å)	15.0–3.25	
Reflections used (free)	52816 (3024)	
R factor	0.224	
R_{free}	0.268	
RMS deviations		
bonds (Å)	0.009	
angles (°)	1.27	
Ramachandran statistics		
most favored (%)	81.4	
additional allowed (%)	17.4	
outliers (%)	0.3	
Model contents		
ErbB2 residues	1123	
pertuzumab residues	872	
sugars	12 NAG, 1 man	

$R_{sym} = \sum_{hkl}|I - \langle I\rangle|/\sum_{hkl} I$ R factor $= \sum_{hkl}||F_{(obs)}| - |F_{(calc)}||/\sum_{hkl}|F_{(obs)}|$

NAG = β-D-N-acetylglucosamine; man = β-D-mannose

The structure of ErbB2 in the ErbB2-pertuzumab complex is very similar to its structure alone and in complex with trastuzumab (Cho et al., 2003). The extracellular domain of ErbB2 is divided into four domains, designated I, II, III, and IV (Figure 1A). I and III are structurally very similar: a repeating sequence of hydrophobic residues, largely leucines, causes these domains to fold into a "β helix" with sides formed by three parallel β sheets. This architecture is distantly related to the classical leucine-rich repeats (Ward and Garrett, 2001). Residues 102–110 form an insertion in the leucine repeat motif of domain I, and are disordered in this structure. Domains II and IV are also similar to each other in structure, being composed of disulfide-bonded modules, small structural units held together by one or two disulfide bonds (Burgess et al., 2003). Domain II contains seven disulfide-bonded modules, with an eighth module being structurally part of domain I. Unlike domain IV, domain II contains an insertion (residues 247–266) in its central disulfide-bonded module which forms a β hairpin that protrudes from

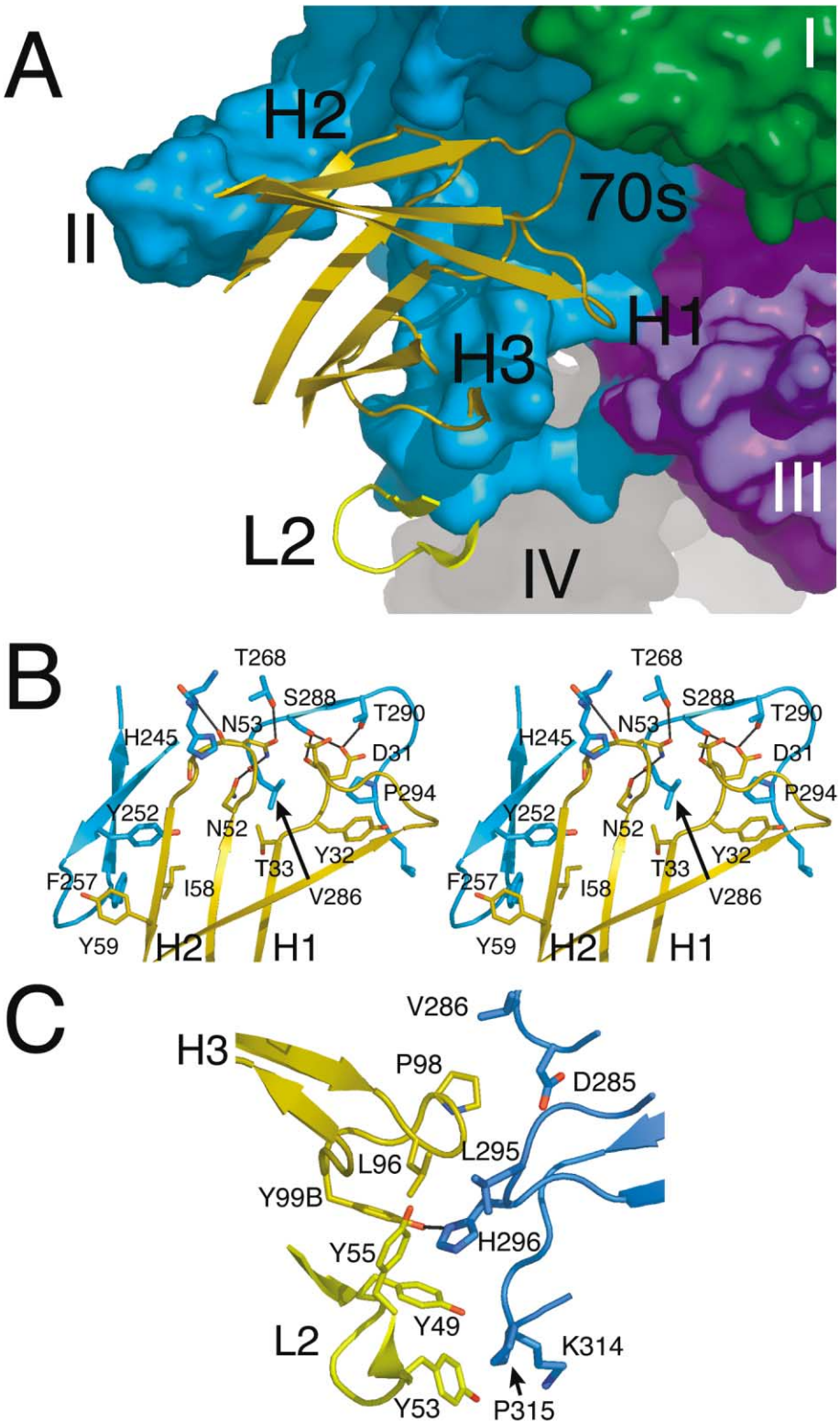

Figure 2. The ErbB2-pertuzumab binding site

A: Overview of the binding site. The four pertuzumab Fab CDRs which interact with ErbB2 are shown in ribbon representation, as is the "70s loop" (heavy chain residues 67–82). ErbB2 is shown in surface form, colored by domain as in Figure 1A.

B: Interactions of CDRs H1 and H2 with ErbB2. Selected residues from ErbB2 and pertuzumab are shown in stick form, with the surrounding backbone in ribbon form. Hydrogen bonds are indicated as black lines. CDRs are labeled near the base of their β hairpins.

C: Interactions of CDRs H3 and L2 with ErbB2. A representation similar to **B**, with heavy chain carbons and ribbons in gold, and light chain in yellow.

the rest of the protein. This β hairpin protrusion is also seen in each monomer of the EGFR homodimer, where it forms one side of the dimerization interface (Garrett et al., 2002; Ogiso et al., 2002). When compared to the structure of ErbB2 alone (Cho et al., 2003), domain IV in the ErbB2-pertuzumab complex is rotated by ~20° relative to the rest of the protein. This domain has little contact with domain III, and is positioned in this crystal primarily by contacts with symmetry-related Fab molecules. Electron density for domain IV steadily deteriorates with increasing distance from domain III, eventually becoming untraceable

after residue 550 (in chain A; 560 in chain B). The ErbB2 in this complex is more heavily glycosylated (~20 kDa of sugar by SDS-PAGE) than the material used in previous crystal structures (Cho et al., 2003), and each of the four N-linked glycosylation sites in the ordered portion of the protein has 1–3 well-ordered sugars attached to it (Figure 1A).

Outside of the complementarity-determining regions (CDRs), pertuzumab is identical in sequence to trastuzumab (Carter et al., 1992); consequently, the local structure of the pertuzumab Fab in the ErbB2-pertuzumab complex is largely the same as that of the trastuzumab Fab, the chief difference being that the elbow angle (the angle between the variable and constant domains of the Fab) is 175°, ~20° larger than in the structure of the trastuzumab Fab (Eigenbrot et al., 1993), and ~30° larger than in the structure of the pertuzumab Fab alone (Vajdos et al., 2002). The conformation of CDR H3 has been substantially altered by binding to ErbB2, compared to the largely similar conformations of this loop in free pertuzumab and in trastuzumab (Eigenbrot et al., 1993; Vajdos et al., 2002). The constant domains of the two pertuzumab Fabs do not obey the same noncrystallographic symmetry as the rest of the complex, being positioned primarily by nonequivalent crystal contacts. The constant domain of one of the two Fabs (chains C and D) is poorly ordered, although the variable domain for this Fab is well ordered.

ErbB2-pertuzumab binding interface

The pertuzumab Fab is bound to ErbB2 near the junction of domains I, II, and III (Figure 1A). This contact buries 1210 Å^2 on the ErbB2 side of the interface, with 1147 Å^2 in domain II and only 63 Å^2 in domain I. Contact is primarily made with the heavy chain of the Fab (878 Å^2 versus 236 Å^2 for the light chain). As expected, most of the ErbB2-pertuzumab contacts involve the CDRs of the Fab, although the dimerization hairpin of domain II lies along the side of the heavy chain variable domain (Figure 2A). Despite the contact with the Fab, the conformation of the dimerization hairpin is essentially the same as that seen in the free and trastuzumab-bound ErbB2 structures as well as that in the EGF receptor dimer: 0.7, 1.0, and 1.3 Å Cα rmsd, respectively, for 59 residues surrounding the β hairpin (Cho et al., 2003; Ogiso et al., 2002).

The interface between ErbB2 and pertuzumab is primarily polar, with few hydrophobic or charged residues in the interface. The largest hydrophobic patch lies outside the main CDR surface, between Ile 58 and Tyr 59 (heavy chain), Tyr 94 (light chain), and Tyr 252 and Phe 257 (ErbB2). (For consistency with previous work on the pertuzumab Fab [Vajdos et al., 2002], we have chosen to use a modified Kabat numbering rather than sequential numbering for pertuzumab residues.) Residues 30–32 on CDR H1 and 52–53 on CDR H2 make an extensive network of hydrogen bonds with main chain and side chain atoms (Figure 2B). His 245 of ErbB2 is tightly sandwiched between Ile 244 and Gly 55 of CDR H2. Although not technically a CDR, the loop containing residues 72–76 makes contacts with ErbB2, including the only contact with domain I, a hydrogen bond between Lys 75 of pertuzumab and Gln 156 of ErbB2. Finally, CDR H3 makes hydrophobic and hydrogen bond contacts with residues Lys 311 and His 296 of ErbB2. His 296 is thoroughly buried upon pertuzumab binding, being surrounded by Tyr 49 and Tyr 55 of the light chain, and Leu 96 and Tyr 99B (modified Kabat numbering) of the heavy chain (Figure 2C).

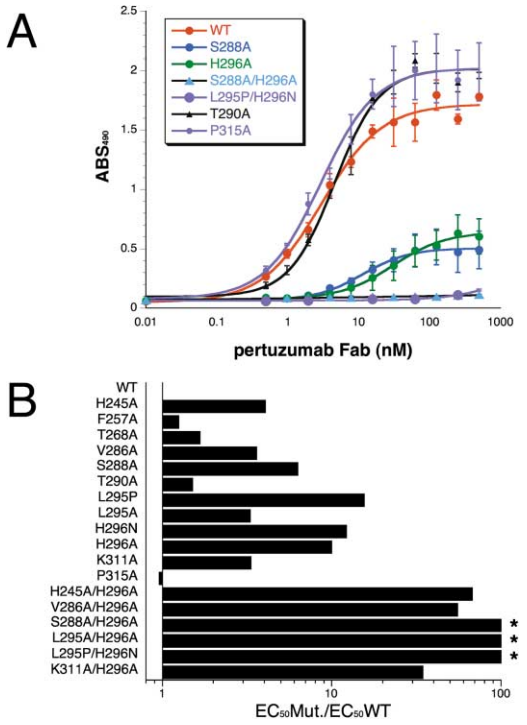

Figure 3. Effect of alanine substitutions on pertuzumab binding to ErbB2

A: Binding of pertuzumab Fab to various ErbB2 mutants was measured by ELISA as described in the Experimental Procedures; curves are shown for wild-type (WT) ErbB2 and for selected mutants with little or no effect (T290A or P315A), a moderate effect (S288A or H296A), or a severe effect (S288A/H296A or L295P/H296N) on pertuzumab binding. Error bars represent the standard error from three experiments.

B: EC_{50} values determined by ELISA for various ErbB2 single and double mutants are shown normalized by the EC_{50} for wild-type ErbB2 (3 nM). The S288A/H296A, L295A/H296A, and L295P/H296N double mutants had no detectable binding to pertuzumab, as indicated by asterisks.

ErbB2 mutagenesis and pertuzumab inhibition

To assess the relative importance of the pertuzumab Fab-ErbB2 binding interactions described above, and to complement previous pertuzumab mutagenesis studies (Vajdos et al., 2002), binding affinities were determined for a number of select ErbB2 mutants. Alanine or other substitutions were made in the context of full-length ErbB2 that was epitope tagged with gD (Paborsky et al., 1990; Schaefer et al., 1999) to allow for verification of expression and to facilitate binding analysis. Recombinant ErbB2 proteins were expressed transiently in COS-7 cells, which were then lysed with nonionic detergent. ErbB2 was then captured from these lysates on anti-gD coated plates. Pertuzumab Fab binding affinities to the captured ErbB2 were measured by ELISA. The EC_{50} for each mutant was determined using a 4-parameter fit of the binding curves (Figure 3A), and these data were used to calculate the EC_{50} ratio for the mutant versus the wild-type (the mut/wt ratio) to give a measure of the severity of each mutation (Figure 3B). Ratios greater than 1 indicate a deleterious mutation. Alanine substitution in any one of residues His 245, Val 286, Ser 288, Leu 295, His 296, or Lys 311 significantly reduces pertuzumab Fab binding affinity for ErbB2, while substitution in residues Phe 257, Thr 268, Thr 290, and Pro 315 results in mut/wt ratios not significantly above 1. Double alanine

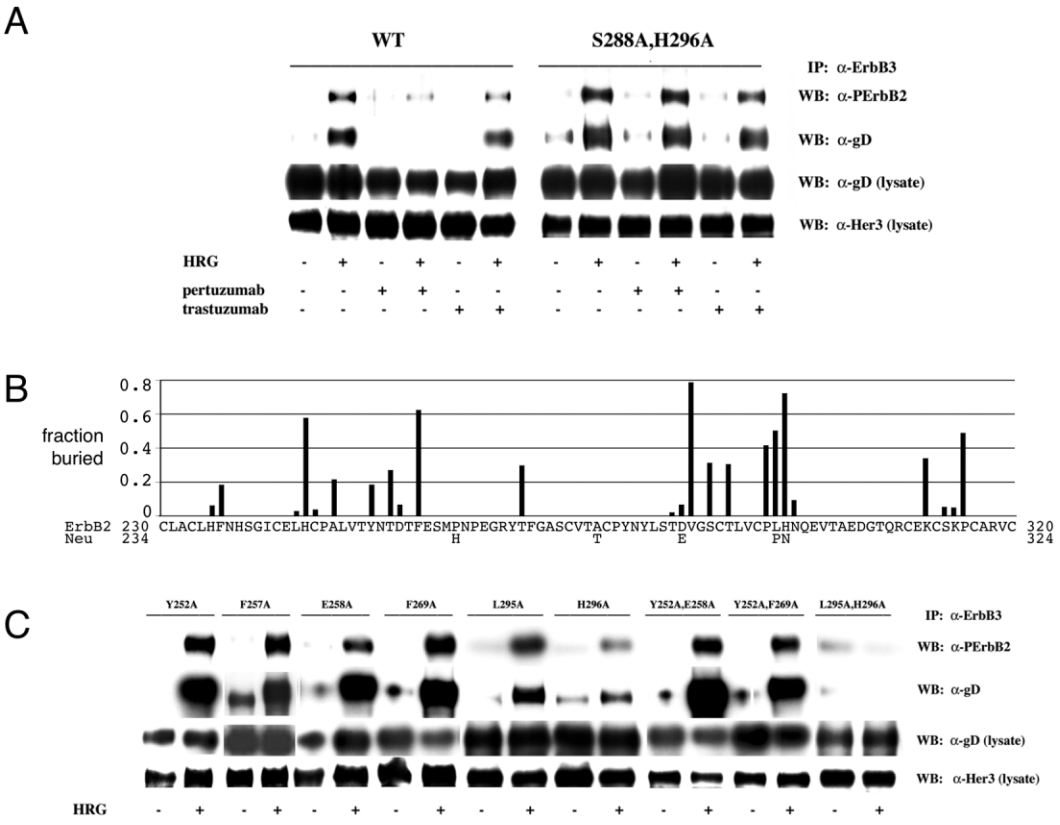

Figure 4. Effect of ErbB2 alanine substitutions on ErbB2-ErbB3 heterodimerization

A: COS-7 cells were cotransfected with ErbB2 wild-type (left panel) or the ErbB2(S288A/H296A) double alanine mutant (right panel) along with ErbB3. Transfected cells were pretreated with or without 100 nM pertuzumab for 1 hr, and stimulated with 2 nM HRG or binding buffer as indicated for 10 min at room temperature. Lysates were prepared and ErbB2-ErbB3 heterodimers were immunoprecipitated with agarose-coupled polyclonal anti-ErbB3 antibody, and ErbB2 receptor activation was evaluated by Western blotting with phosphospecific anti-ErbB2 antibody (α-PErbB2), or anti-gD antibody (α-gD) to detect ErbB2-ErbB3 complexes. Lysates were evaluated for expression of ErbB2 and ErbB3 construct expression with anti-gD or anti-ErbB3 (α-ErbB3) antibodies, respectively.

B: A sequence alignment of human ErbB2 and neu is shown for a portion of domain II. The bars above each residue indicate the fraction of the side chain solvent-accessible surface area, which is buried upon pertuzumab binding.

C: COS-7 cells were cotransfected with alanine mutant ErbB2 and wild-type ErbB3 expression plasmids, stimulated with 2 nM HRG for 10 min at room temperature, and assayed for HRG-dependent ErbB2 phosphorylation and heterodimerization in a coimmunoprecipitation assay similar to that presented in **A**.

substitutions in contact residues 245/296, 286/296, or 311/296 reduce binding further, and the 288/296 double mutation lacks any detectable binding to pertuzumab Fab in this assay. In addition, the pertuzumab Fab is unable to prevent HRG-dependent heterodimerization of the 288/296 double mutant ErbB2 with ErbB3 (Figure 4A). In agreement with our previous studies (Agus et al., 2002), trastuzumab has little effect on ErbB2-ErbB3 heterodimerization.

Specificity of pertuzumab for human ErbB2

Pertuzumab is specific for human ErbB2 and does not bind to rodent ErbB2 (neu) with detectable affinity (Fendly et al., 1990). There are five residues in domain II which differ between human and rat ErbB2, and only two (Leu 295 and His 296) make significant side chain contacts with the pertuzumab Fab (Figure 4B**)**. Substitution of residues L295 and/or H296 in ErbB2 with neu residues (L295P, H296N, or L295P/H296N) is sufficient to eliminate detectable binding to pertuzumab (Figure 3B). These substitutions also reduce the ability of pertuzumab to inhibit HRG-dependent receptor phosphorylation. While pertuzumab can block HRG-dependent activation in wild-type ErbB2 transfected cells, inhibition is not observed in ErbB2(L295P/H296N) transfected cells (Supplemental Figure S1 as http://www.cancercell.org/cgi/content/full/5/4/317/DC1).

ErbB2 heterodimerization with ErbB3 and the pertuzumab binding site

A number of ErbB2 residues in and around the pertuzumab binding site are homologous to EGFR residues necessary for homodimerization (Ogiso et al., 2002). To test the importance of these residues in an ErbB2/ErbB3 heterodimer, alanine substitutions were made at ErbB2 residues Tyr 252, Phe 257, Glu 258, Phe 269, Leu 295, and His 296 corresponding respectively to EGFR residues Tyr 246, Tyr 251, Gln 252, Phe 263, Ala 289, and Asp 290; the ErbB2 double mutants Y252A/E258A, Y252A/F263A, and L295A/H296A were also tested. Only the L295A/H296A double mutant was able to impair HRG-dependent receptor ErbB2-ErbB3 heterodimerization (Figure 4C), although

smaller effects on heterodimerization could very well be below the sensitivity limits of our assay. None of the other pertuzumab contact single alanine mutations discussed above had any effect on ErbB2 heterodimerization (Supplemental Figure S2).

Discussion

Pertuzumab binds at the ErbB2 heterodimerization interface

The central portions of domain II in ErbB2 and EGFR are highly homologous and represent the majority of the dimerization interface observed in EGFR (Garrett et al., 2002; Ogiso et al., 2002). Since this region overlaps with the binding epitope of pertuzumab (Figure 5A), an analysis of residues in this area should shed light on both pertuzumab binding and ErbB2 dimerization. Surface-exposed residues on pertuzumab and ErbB2 can be part of one or both of two binding epitopes: a structural epitope, defined by the contacts between the two molecules, and a functional epitope, determined by previous mutagenesis of the pertuzumab Fab (Vajdos et al., 2002) and our mutagenesis of ErbB2. The overlap between these two epitopes (Figure 5) defines the essential contacts between pertuzumab and ErbB2.

Pertuzumab's light and heavy chains play different roles in ErbB2 binding

The light chain of the pertuzumab Fab makes only a few contacts with ErbB2, mostly via CDR L2, and none of the contact residues affects ErbB2 binding when mutated (Vajdos et al., 2002). Conversely, light-chain residues which do affect binding when mutated do so indirectly, since none of these residues contacts ErbB2 (Figure 5B). The picture is quite different for the pertuzumab heavy chain, where 24 residues contact ErbB2 directly; seven of these affect binding by at least 75-fold when mutated (Figure 5B). These essential residues form an extensive hydrogen bond network with ErbB2, as discussed previously (Figure 2B), and occupy a compact patch on the surface of the pertuzumab Fab. Vajdos et al. (2002) observed a similar, if less compact, patch from their mutagenic analysis of the pertuzumab Fab alone.

Certain residues of ErbB2 are essential for pertuzumab binding and heterodimerization

On the ErbB2 side of the interface, the S288A mutant is 6-fold weaker in pertuzumab binding, probably due to the loss of the hydrogen bonds between Ser 288 of ErbB2 and Asp 31 of the Fab. In contrast, Thr 290 also hydrogen bonds to Asp 31, yet the T290A mutant has almost no detectable loss in pertuzumab binding. While our limited resolution prevents any detailed analysis of hydrogen bonds, Ser 288 does make two hydrogen bonds to pertuzumab, while Thr 290 only makes one, perhaps explaining the different effects of these mutations. The double alanine substitutions V286A/H296A and L295A/H296A have dramatic effects on pertuzumab binding due to the loss of multiple hydrophobic interactions with the Fab, as well as the hydrogen bond to Tyr 99B. Additionally, pertuzumab will not bind to rodent ErbB2 (Fendly et al., 1990), probably due to the substitution of a proline for Leu 295 and an asparagine for His 296. Indeed, the L295P/H296N double mutant of human ErbB2 is severely impaired in pertuzumab binding. The patch of pertuzumab residues necessary for ErbB2 binding (Figure 5B) is mirrored by a cluster of ErbB2 residues important for pertuzumab binding (Figure 5A), confirming that our structure has captured

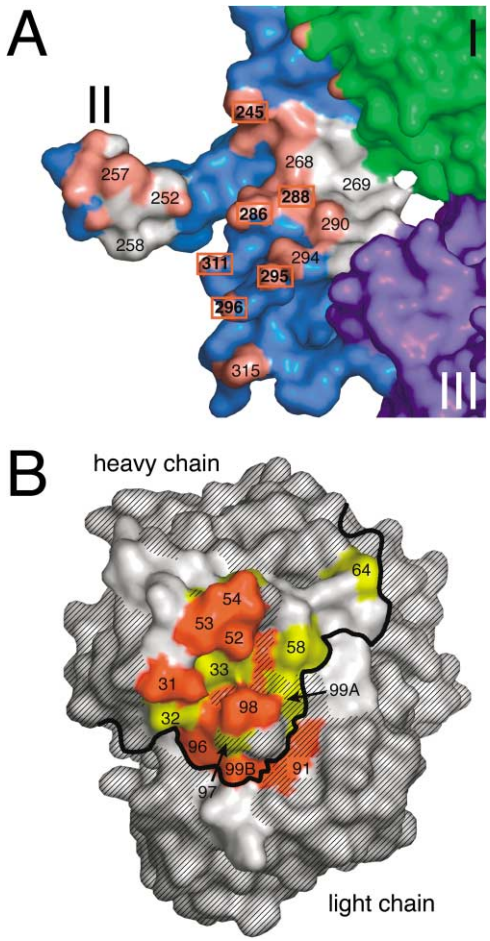

Figure 5. The ErbB2 and pertuzumab binding epitopes

A: Overlap of dimerization and pertuzumab binding sites. ErbB2 is shown in surface representation, colored as in Figure 1A. ErbB2 residues homologous to those EGFR residues which contact the dimerization hairpin are shown in white (some atoms may be colored pink due to pertuzumab contact). Individual atoms in ErbB2 which directly contact pertuzumab atoms (<3.2 Å distance) are shown in pink. ErbB2 residues mentioned in the text are labeled; those that inhibit pertuzumab binding when mutated to alanine are boxed in red.

B: Overlap of the structural and functional ErbB2 binding regions. The molecular surface of the pertuzumab Fab is shown in an open book orientation relative to **A** (i.e., the right side of **B** folds on top of the left side of **A**, so that pertuzumab residue 64 contacts the tip of the dimerization hairpin of ErbB2). Residues which do not contact ErbB2 are hatched. Residues which displayed a >75-fold loss in binding to ErbB2 when mutated to alanine (Vajdos et al., 2002) are colored red; residues with a 10- to 75-fold loss in binding are colored yellow. The heavy black line separates the heavy chain (upper left) from the light chain (lower right) of the Fab.

the functionally relevant ErbB2-pertuzumab complex. To date, mutations similar to the ones we have tested have not been reported in ErbB2 isolated from cancer patients.

Pertuzumab Fab sterically interferes with ErbB2 heterodimerization

Our structure provides a clear explanation for the inhibition of ErbB2-mediated signaling by pertuzumab, and validates the model of ErbB2 heterodimerization based on the structure of the EGFR homodimer (Figures 6A–6H). The pertuzumab binding epitope overlaps with a region which, by modeling and by ho-

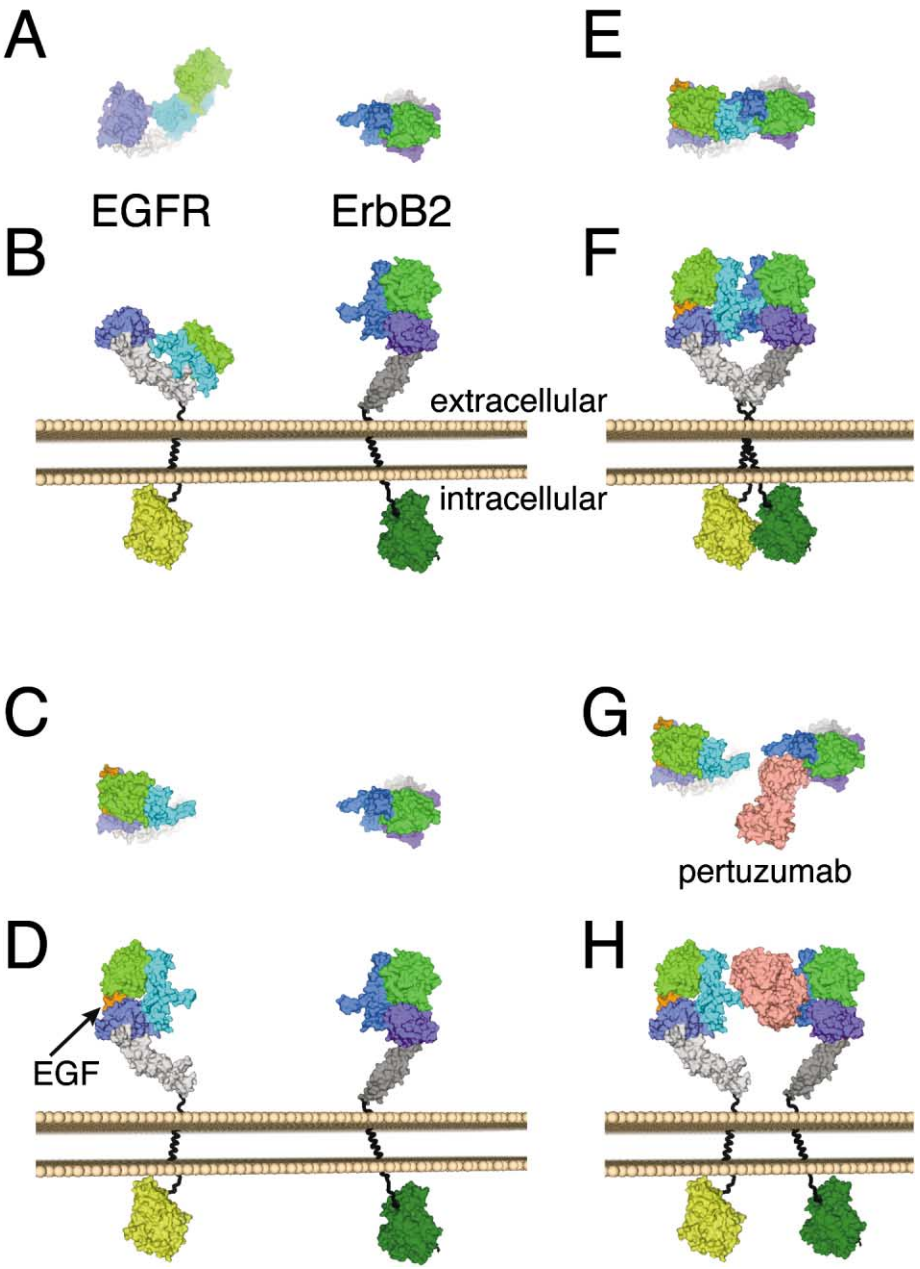

Figure 6. ErbB2 heterodimerization and pertuzumab interference

Top-down (**A**, **C**, **E**, and **G**) and side (**B**, **D**, **F**, and **H**) views of various states of the EGFR-ErbB2 heterodimerization process, modeled as described in the Experimental Procedures. EGFR and ErbB2 extracellular domains are shown in surface representation, with EGFR and ErbB2 domains I in green, II in blue, III in purple, and IV in gray. EGFR is always on the left of the panel, and ErbB2 on the right. EGF, when present, is shown as an orange surface, while pertuzumab (**G** and **H**) is shown as a pink surface. The lipid bilayer is represented as tan spheres, with the modeled transmembrane helices as black tubes. The dimerization of the intracellular kinase domains of EGFR (yellow surface) and ErbB2 (dark green surface) is not meant to suggest the orientation of the actual kinase dimer.

A and B: The closed (ligand-free) form of EGFR is modeled near a molecule of ErbB2. In its unliganded form, the extracellular domain of EGFR (or ErbB3) is in a conformation which cannot dimerize with another receptor (Cho and Leahy, 2002; Ferguson et al., 2003).

C and D: EGFR is now shown in its open, ligand-bound state. Upon binding a ligand such as EGF, EGFR rearranges into a conformation which exposes the dimerization hairpin, shown protruding from the center of domain II in light blue.

E and F: EGFR and ErbB2 are now heterodimerized. The two receptors interact via each one's dimerization hairpin, the membrane-proximal portion of domain IV, and (at least in this model) the transmembrane helices and intracellular kinase domains. ErbB2 heterodimers with EGFR, ErbB3, and ErbB4 are all expected to look identical at this level of detail.

G and H: Pertuzumab has bound to ErbB2, blocking heterodimerization by preventing the EGFR dimerization hairpin from fitting in its binding pocket on ErbB2.

mology with EGFR, is expected to be the binding site for the dimerization hairpin (Figures 5A and 6F); therefore, bound pertuzumab is modeled to sterically prevent the dimerization hairpin from reaching its binding pocket (Figures 6G–6H). The fact that pertuzumab binding inhibits ErbB2 heterodimerization (Agus et al., 2002) can now be interpreted in light of our structure as experimental evidence supporting this dimerization model. Pertuzumab Fab bound to domain II would not sterically interfere with other dimerization contacts, such as those in domain IV (Figure 6F); if the dimerization hairpin could bend out of the way, a receptor heterodimer could still potentially be formed. The conformation of this hairpin is nearly identical in all three ErbB2 structures as well as the two EGFR homodimer structures (Cho et al., 2003; Garrett et al., 2002, 2003; Ogiso et al., 2002), suggesting that the hairpin is quite rigid and that sterically blocking the hairpin binding pocket is in fact sufficient to prevent ErbB2 heterodimerization. Our structure shows that the presence of the entire pertuzumab antibody is not needed to cause this steric interference; the Fab fragment alone is sufficient, in agreement with our previous studies (Agus et al., 2002).

ErbB2 heterodimerization appears to be different than EGFR homodimerization

By binding to ErbB2 domain II, pertuzumab occludes a number of residues which likely contact the other ErbB receptor in the heterodimer (Figure 5A). We questioned which, if any, of these residues was important for heterodimerization, and in particular whether mutations in this region have the same deleterious effects in an ErbB2/ErbB3 heterodimer as they have been shown to have in an EGFR homodimer (Ogiso et al., 2002). In EGFR,

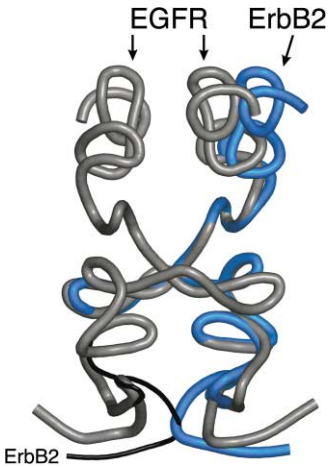

Figure 7. Altered conformation of ErbB2 domain II

The two copies of domain II (residues 188–313) from the EGFR dimer structure are shown as gray tubes. Domain II (residues 195–320) from ErbB2, superimposed on the central disulfide-bonded modules as described in the text, is shown as a blue tube. The last two disulfide-bonded modules from a copy of ErbB2 superimposed on the other EGFR monomer are shown as a black line to indicate the potential steric clash in this region. For clarity in this figure, the Cα backbone traces have been heavily smoothed.

residues Tyr 246 and Arg 285 interact across the dimer interface, as do Tyr 251 and Phe 263 (Garrett et al., 2002; Ogiso et al., 2002). ErbB2 substitutes a leucine (Leu 291) for Arg 285 in EGFR, breaking the first of these interactions. Therefore, the ErbB2 mutations F257A and F269A, neither of which affects ErbB2/ErbB3 heterodimerization, are analogous to the EGFR double mutants R285S/Y251A and R285S/F263A, which completely eliminate EGFR homodimerization (Ogiso et al., 2002). Other residues in this region of ErbB2 can also be mutated to alanine with no effect on ErbB2/ErbB3 heterodimerization. Thus, our mutagenesis suggests that formation of ErbB2 heterodimers may be less dependent on correct contacts with the dimerization arm than formation of EGFR homodimers.

Altered conformation of ErbB2 domain II suggests a novel heterodimer contact

The conformation of ErbB2 is similar to that of activated, dimeric EGFR; however, small but significant differences in the shape of domain II may explain the different dimerization properties of these two receptors. Domain II of the ErbB receptors is rather like a spine, with rigid "vertebrae" (the disulfide-bonded modules) held in an overall conformation by domains I and III; these domains differ in orientation between EGFR and ErbB2 due to the lack of an ErbB2 ligand (Figure 6D). As a result, the N-terminal portion of ErbB2 domain II is farther from the modeled dimer interface than in EGFR, while the C-terminal portion is closer (Figure 7). The last two disulfide-bonded modules of EGFR domain II do not make significant dimer contacts in either EGFR homodimer structure, with Cα-Cα distances no less than 10 Å (Garrett et al., 2002; Ogiso et al., 2002). In the modeled ErbB2 heterodimer, this region is now in direct contact with the other receptor, with a Cα-Cα distance as low as 4.5 Å. His 296 is in this region, and has been placed relatively close to a conserved aspartate (residue 279 in EGFR, ErbB3, and ErbB4; residue 288 in ErbB2) in the modeled dimer partner, possibly explaining the effects of the L295A/H296A mutation on heterodimerization. The structure of this region is essentially the same in Neu as in human ErbB2 (Cho et al., 2003), and Asn 296 in Neu could make the same dimer interactions that His 296 does in our model. An unresolved issue is that the single mutants, L295A and H296A, show little or no effect on heterodimerization, although we suspect that these mutants may have a small deleterious effect which is below the sensitivity limits of our heterodimerization assay. Taken together, these structural and mutational data suggest that the C-terminal portion of ErbB2 domain II is involved in heterodimerization, and that some residues in this region, in particular Leu 295 and His 296, are important for heterodimerization as well as pertuzumab binding.

Interestingly, an ErbB2 homodimer cannot be modeled in the same way as the ErbB2 heterodimer discussed above. The last two disulfide-bonded modules of ErbB2 domain II would be too close to the dimer interface, interpenetrating by more than 6 Å in the region of Ser 313 (Figure 7). At minimum, resolving this steric clash would require reorienting the two ErbB2 molecules, possibly disrupting interactions involving the dimerization hairpin or domain IV. This clash may combine with electrostatic repulsion between ErbB2 monomers (Garrett et al., 2003) and loss of interactions with the dimerization hairpin (Cho et al., 2003) to explain why the extracellular domain of ErbB2 will not homodimerize in solution (Ferguson et al., 2000); all of these effects arise from the differences in domain II which give ErbB2 a unique role as a heterodimerization partner.

In conclusion, our present study provides a satisfying structural basis for pertuzumab's effect as a heterodimerization inhibitor. Bound pertuzumab occludes the pocket on ErbB2 that would accept the dimerization hairpin of a heterodimer partner, preventing the association of the two receptors and subsequent growth signaling. Pertuzumab therefore represents a novel class of targeted therapeutic agents, those that inhibit ErbB2's function as a coreceptor. The ErbB2-pertuzumab complex suggests that alternative antibodies, antibody fragments, or peptidomimetics could also function as heterodimerization inhibitors. Recently, pertuzumab has successfully completed phase I clinical testing. These studies suggest that the ErbB2 heterodimerization inhibitor can be given safely to patients with advanced malignancies; in addition, pertuzumab produced an objective response in some of these patients, all of whom had failed to respond to one or more prior treatment programs. Ongoing phase II proof-of-concept studies will determine whether inhibition of ErbB2 heterodimerization warrants further development in patients whose tumors lack ErbB2 gene amplification, but are instead driven by ligand-activated ErbB2.

Experimental procedures

Cloning and expression

Residues 1–624 of the extracellular domain of ErbB2 were stably expressed and secreted in CHO cells as previously described (Hudziak and Ullrich, 1991). Conditioned media (100 liter), with an estimated ErbB2 concentration ~15 mg/L, was concentrated to 12 liter and frozen at −70° C for further processing. Pertuzumab is built on the same antibody framework as trastuzumab (Carter et al., 1992). Selection and humanization of the pertuzumab antibody will be described elsewhere (C. Adams, D. Allison, J. Clark, B. Fan, T. Breece, C. Schmelzer, S. Brignoli, K. Totpal, G. Phillips, L. Presta, and M.X.S., unpublished data). The heavy and light chains of the pertuzumab Fab fragment were coexpressed into the periplasm of the 33B6 strain of *E. coli* under the control of an alkaline phosphatase promoter, using an expres-

sion system originally developed for an anti-LFA-1 Fab (Werther et al., 1996). Cells (1900 g) were harvested from a 10 liter fermentation and frozen at −70° C in ~200 g batches.

Protein purification

ErbB2 extracellular domain (ECD) was purified by immunoaffinity and gel filtration chromatography. A trastuzumab affinity column was prepared by coupling 400 mg trastuzumab (intact MAb; Genentech, Inc.) to 40 g CNBr-activated sepharose (Pharmacia); the resulting 100 ml column has the capacity to bind at least 200 mg of ErbB2 ECD. Concentrated ErbB2 ECD from conditioned CHO cell medium was applied to the trastuzumab column, eluted with 10 mM HCl, and immediately neutralized with 1 M Tris (pH 8.0). Fractions containing ErbB2 ECD were concentrated and passed over a Superdex-200 column (Pharmacia) to separate monomeric protein from disulfide-linked aggregates. The purified protein was stored at 4°C in PBS + 0.02% sodium azide.

Pertuzumab Fab was also purified by affinity and gel filtration chromatography. Briefly, the Fab was released from *E. coli* cells using osmotic shock by resuspending frozen cells in 0.1 M acetic acid (pH ~3), 25 mM EDTA, 1 mM PMSF. Impurities were removed from the shockate by batch binding to DEAE-sepharose (Pharmacia) at 0.5 ml resin per gram of cells. The processed shockate was then passed over a protein G-sepharose column (Pharmacia) to trap the Fab, and the column was then washed with 10 mM MES (pH 5.5), 10 mM EDTA. Bound Fab was subsequently eluted with 0.1 M acetic acid, and the eluate was neutralized with 1 M Tris (pH 8.0). The pooled Fab-containing fractions were further purified by Superdex-200 gel filtration. Purified pertuzumab Fab, like purified ErbB2 ECD, is very stable in PBS + 0.02% sodium azide. Early crystallization trials used protein produced by a different method (Vajdos et al., 2002); however, the crystals were identical to those described here.

ErbB2-pertuzumab complex preparation and crystallization

ErbB2 (10.5 mg at 3.5 mg/ml) and pertuzumab Fab (10.1 mg at 1.3 mg/ml) were mixed (a 33% molar excess of pertuzumab) and allowed to incubate overnight at 4°C. The complex was then separated from excess pertuzumab Fab by running over a Superdex-200 column in PBS. The purified complex was concentrated to 10 mg/ml and stored for crystallization in 25 mM Tris (pH 8.0), 150 mM NaCl, 0.1 mM EDTA.

The purified ErbB2-pertuzumab complex was mixed 1:1 with well solution (22% PEG 3350, 100 mM ammonium formate) and equilibrated by hanging- or sitting-drop vapor diffusion against the well solution. The pH of this mother liquor is not well defined, since there is no buffering capacity at neutral pH except for the residual Tris from the protein storage solution; however, the pH of 100 mM ammonium formate is ~6.5. Tetragonal bipyramids appear in a few days and grow to 100–200 micron size in a week. Crystals were removed from their mother liquor and cryostablized in 100 mM ammonium formate, 25% PEG 3350, 20% ethylene glycol, then frozen in liquid nitrogen.

Data collection and structure determination

Data for the ErbB2-pertuzumab complex were collected at Beamline 5.0.1 of the Advanced Light Source (Berkeley). Highly redundant data were collected to help counteract the generally weak diffraction. Data statistics are shown in Table 1. A molecular replacement solution for the ErbB2 portion of the complex was obtained using AMoRe (Navaza, 1994), with the structure of rat ErbB2 (Cho et al., 2003) as a search model. Once both ErbB2 molecules in the asymmetric unit were found, further molecular replacement using the variable domain of the pertuzumab Fab (Vajdos et al., 2002) identified the location of the two pertuzumab molecules. Initial rigid-body refinement of the various domains of the complex was performed using CNX (Accelrys, Inc.) without enforcing the noncrystallographic symmetry. Subsequent positional and restrained individual atomic B factor refinement was performed using CNX and Refmac5 (Murshudov et al., 1997), with fairly tight NCS restraints to prevent overrefinement. Model statistics are in Table 1.

Modeling of an ErbB2 heterodimer

Modeling of an ErbB2-containing heterodimer used the EGFR homodimer structure (Ogiso et al., 2002) as a starting point, with ErbB2 superimposed onto one of the two EGFR molecules. Because of the altered global conformation of ErbB2 versus EGFR, a global superposition of the two molecules is quite poor (Cα rmsd ~6 Å). Superposition by domain lowers the Cα rmsd to 2–3 Å depending on the domain, but raises the question of which superposition to use for the modeling. Since nearly all of the dimerization contacts in EGFR lie in domain II, this is the logical choice for superposition when making a heterodimer model. Further analysis (see Discussion and Figure 7) shows that only residues 232–292 of ErbB2 (EGFR residues 226–286) should be included in the superposition. These residues superimpose well, with a Cα rmsd of 1.3 Å (excluding only two residues at the tip of the dimerization hairpin). Domain IV of EGFR is disordered or not present in the dimeric EGFR structures (Garrett et al., 2002; Ogiso et al., 2002), but can be plausibly inferred by superposition of domains III and IV from the closed form of EGFR (Ferguson et al., 2003) onto domain III of the dimeric form. This superposition places the C termini of the modeled extracellular domains of EGFR and ErbB2 in close proximity, allowing the modeled transmembrane helices to associate. Transmembrane helices and linker peptides were created de novo, and two copies of the kinase domain of EGFR (Stamos et al., 2002) were placed next to each other in an arbitrary orientation, not one of the previously proposed ErbB kinase dimer models (Groenen et al., 1997; Murali et al., 1996).

While there is no structure of ErbB3 in its ligand-bound, active form, the inactive forms of EGFR and ErbB3 show a remarkable similarity to one another, with Cα rmsds for domains I, III, and IV of 0.9–1.2 Å (and 1.9 Å for domain II). To a first approximation, therefore, an EGFR/ErbB2 heterodimer model will be identical to an ErbB3/ErbB2 heterodimer model, with the caveat that the heterodimerized conformation of ErbB3 (or EGFR) may not be the same as that of homodimeric EGFR.

ErbB2 mutagenesis and COS-7 transfections

All wild-type and ErbB2 mutant constructs used in this study were epitope-tagged at the N terminus with the herpes simplex virus signal sequence of gD replacing the endogenous ErbB2 signal sequence (Schaefer et al., 1999). Mutations were introduced into a 1.5 Kb EcoR1-XhoI restriction fragment of ErbB2 in pBSKS- (Stratagene) using the Quick-change method following manufacturer's recommendations (Stratagene). Mutants were then subcloned into the EcoRI-XhoI site of full-length gDErbB2 in a pRK5 mammalian expression vector. All mutations were confirmed by automated DNA sequencing. COS-7 cells (1×10^6 cells/10 cm dish) were transfected with 1 μg of pRK5.gDErbB2 wild-type or pRK5.gDErbB2 mutant DNA with or without 10 μg of pRK7.ErbB3 DNA as described using LipofectAMINE according to the manufacturer's recommendations (Invitrogen). Twenty-four hours post-transfection, cells were serum starved overnight in 0.1% fetal bovine serum/DMEM at 37°C prior to treatment.

Pertuzumab binding assays

The relative affinity of pertuzumab Fab for ErbB2 or ErbB2 mutants was measured by ELISA. COS-7 cells were transfected with 10 μg of pRK5.gDErbB2 or pRK5.gDErbB2 mutant plasmids. After 24 hr, cells were lysed in 1 ml of lysis buffer (1% Triton X-100, 1% CHAPS, 25 mM Tris [pH 8.0], 150 mM NaCl, 0.5 mM PMSF, 10 U/ml aprotinin, and 10 μg/ml leupeptin). Lysates were normalized to 1 ng/ml gDErbB2 protein using the purified soluble extracellular domain of ErbB2 as a standard (Vajdos et al., 2002) as quantified by an ORIGEN assay using 2 μg/ml biotinylated anti-gD antibody 5B6 for capture and 0.5 μg/ml ori-tagged trastuzumab for detection via an Origen analyzer following manufacturer's instructions (IGEN).

Nunc maxisorp plates (Nunc) were coated with 5 μg/ml anti-gD tag capture antibody (3C8) in PBS overnight at 4°C, and blocked for two hours with 5% bovine serum albumin (Sigma) in PBS. Normalized lysates were added to coated ELISA plates and allowed to bind for 2 hr at 4°C. Plates were rinsed with PBS/0.1% Tween 20, and serial dilutions of purified pertuzumab Fab were added to the plates in PBS and allowed to bind for 2 hr. Plates were rinsed with PBS/0.1% Tween 20, and an anti-human Fab-specific HRP conjugated antibody (Biosource) was added at 1/5000 dilution in PBS/1% BSA/0.1% Tween for 1 hr. Plates were rinsed 6× with PBS/0.1% Tween, and bound gDErbB2 was detected using TMB as a substrate (Sigma) and measured at 490 nm using a plate reader. The EC_{50} for each mutant was calculated from the binding curves using a 4 parameter fit function, and relative affinities were estimated by dividing the EC_{50} of each mutant by the EC_{50} of wild-type gDErbB2.

Coimmunoprecipitation assays

Activation of ErbB2 was evaluated by heterodimerization with ErbB3 upon heregulin (HRG) stimulation in a coimmunoprecipitation assay (Agus et al., 2002). Prior to stimulation, the medium was changed to fresh DMEM with or without 100 nM pertuzumab or trastuzumab for 1 hr prior to stimulation as indicated. COS-7 cells were stimulated for 10 min at room temperature with 2 nM of recombinant heregulin ($HRG\beta1_{177-244}$), in binding buffer (RPMI medium, 0.02% BSA, 10 mM Hepes [pH 7.2]) or binding buffer alone as described. Transfected cells were lysed in 1 ml RPMI lysis buffer (1% v/v Triton X-100, 1% w/v CHAPS, 10 mM HEPES (pH 7.2), in RPMI medium containing 0.2 mM PMSF, 10 μg/ml leupeptin, 10 U/ml aprotinin, and 1 mM Na_3VO_4). Heterodimers were immunoprecipitated from 500 μl of lysate using rabbit polyclonal anti-ErbB3 antibody (Santa Cruz) covalently coupled to agarose (Pierce ultralink) at 4°C for 2 hr. Complexes were washed twice in lysis buffer and resuspended in SDS sample buffer and boiled. Samples were separated on a 4%–12% polyacrylamide gel (Novex) and electroblotted onto nitrocellulose membranes. Blots were blocked in 5% BSA/TBST and probed with either phosphospecific anti-ErbB2 antibody (Neomarkers), or an anti-gD epitope monoclonal antibody (5B6) to detect gDErbB2 followed by a peroxidase-conjugated anti-mouse secondary antibody (Amersham). To verify and normalize for expression of transfected constructs between experimental conditions, 50 μg of cell lysate was checked by Western blotting with anti-gD antibody (5B6) or anti-ErbB3 (Ab7, Neomarkers) antibody. Anti-mouse HRP-conjugated secondary antibody was used for visualization by enhanced chemiluminescence (ECL, Amersham Pharmacia Biotech).

Phosphorylation assays

Pertuzumab inhibition of HRG-dependent activation of gDErbB2 or gDErbB2 mutants was detected by a tyrosine phosphorylation assay as previously described (Schaefer et al., 1999).

Acknowledgments

We wish to thank M. Ultsch, S. Hymowitz, C. Wiesmann, and J. Stamos for help with data collection, and C. Eigenbrot and D. Sidhu for insightful comments and feedback during preparation of this manuscript. We also wish to thank the DNA synthesis and sequencing groups at Genentech for their support on this project. Our data collection was facilitated by Thomas Earnest of the Advanced Light Source, which is supported by the Director, Office of Science, Office of Basic Energy Sciences, Materials Sciences Division, of the U.S. Department of Energy under Contract No. DE-AC03-76SF00098 at Lawrence Berkeley National Laboratory. M.C.F., K.D.C., A.M.dV., and M.X.S. are employees of, and stockholders in, Genentech, Inc., the maker of the drugs pertuzumab and trastuzumab.

Received: October 14, 2003
Revised: February 9, 2004
Accepted: February 26, 2004
Published: April 19, 2004

References

Agus, D.B., Akita, R.W., Fox, W.D., Lofgren, J.A., Higgins, B., Maiese, K., Scher, H.I., and Sliwkowski, M.X. (2000). A potential role for activated HER-2 in prostate cancer. Semin. Oncol. *27*, 76–83.

Agus, D.B., Akita, R.W., Fox, W.D., Lewis, G.D., Higgins, B., Pisacane, P.I., Lofgren, J.A., Tindell, C., Evans, D.P., Maiese, K., et al. (2002). Targeting ligand-activated ErbB2 signaling inhibits breast and prostate tumor growth. Cancer Cell *2*, 127–137.

Aroian, R.V., Koga, M., Mendel, J.E., Ohshima, Y., and Sternberg, P.W. (1990). The let-23 gene necessary for Caenorhabditis elegans vulval induction encodes a tyrosine kinase of the EGF receptor subfamily. Nature *348*, 693–699.

Arteaga, C.L. (2003). ErbB-targeted therapeutic approaches in human cancer. Exp. Cell Res. *284*, 122–130.

Burgess, A.W., Cho, H.S., Eigenbrot, C., Ferguson, K.M., Garrett, T.P., Leahy, D.J., Lemmon, M.A., Sliwkowski, M.X., Ward, C.W., and Yokoyama, S. (2003). An open-and-shut case? Recent insights into the activation of EGF/ErbB receptors. Mol. Cell *12*, 541–552.

Carter, P., Presta, L., Gorman, C.M., Ridgway, J.B., Henner, D., Wong, W.L., Rowland, A.M., Kotts, C., Carver, M.E., and Shepard, H.M. (1992). Humanization of an anti-p185HER2 antibody for human cancer therapy. Proc. Natl. Acad. Sci. USA *89*, 4285–4289.

Carter, P., Fendly, B.M., Lewis, G.D., and Sliwkowski, M.X. (2000). Development of Herceptin. Breast Disease *11*, 103–111.

Cho, H.S., and Leahy, D.J. (2002). Structure of the extracellular region of HER3 reveals an interdomain tether. Science *297*, 1330–1333.

Cho, H.S., Mason, K., Ramyar, K.X., Stanley, A.M., Gabelli, S.B., Denney, D.W., Jr., and Leahy, D.J. (2003). Structure of the extracellular region of HER2 alone and in complex with the Herceptin Fab. Nature *421*, 756–760.

Clynes, R.A., Towers, T.L., Presta, L.G., and Ravetch, J.V. (2000). Inhibitory Fc receptors modulate in vivo cytoxicity against tumor targets. Nat. Med. *6*, 443–446.

Cobleigh, M.A., Vogel, C.L., Tripathy, D., Robert, N.J., Scholl, S., Fehrenbacher, L., Wolter, J.M., Paton, V., Shak, S., Lieberman, G., and Slamon, D.J. (1999). Multinational study of the efficacy and safety of humanized anti-HER2 monoclonal antibody in women who have HER2-overexpressing metastatic breast cancer that has progressed after chemotherapy for metastatic disease. J. Clin. Oncol. *17*, 2639–2648.

Eigenbrot, C., Randal, M., Presta, L., Carter, P., and Kossiakoff, A.A. (1993). X-ray structures of the antigen-binding domains from three variants of humanized anti-p185HER2 antibody 4D5 and comparison with molecular modeling. J. Mol. Biol. *229*, 969–995.

Falls, D.L. (2003). Neuregulins: functions, forms, and signaling strategies. Exp. Cell Res. *284*, 14–30.

Fendly, B.M., Winget, M., Hudziak, R.M., Lipari, M.T., Napier, M.A., and Ullrich, A. (1990). Characterization of murine monoclonal antibodies reactive to either the human epidermal growth factor receptor or HER2/neu gene product. Cancer Res. *50*, 1550–1558.

Ferguson, K.M., Darling, P.J., Mohan, M.J., Macatee, T.L., and Lemmon, M.A. (2000). Extracellular domains drive homo- but not hetero-dimerization of erbB receptors. EMBO J. *19*, 4632–4643.

Ferguson, K.M., Berger, M.B., Mendrola, J.M., Cho, H.S., Leahy, D.J., and Lemmon, M.A. (2003). EGF activates its receptor by removing interactions that autoinhibit ectodomain dimerization. Mol. Cell *11*, 507–517.

Fry, D.W. (2003). Mechanism of action of erbB tyrosine kinase inhibitors. Exp. Cell Res. *284*, 131–139.

Garrett, T.P., McKern, N.M., Lou, M., Elleman, T.C., Adams, T.E., Lovrecz, G.O., Zhu, H.J., Walker, F., Frenkel, M.J., Hoyne, P.A., et al. (2002). Crystal structure of a truncated epidermal growth factor receptor extracellular domain bound to transforming growth factor alpha. Cell *110*, 763–773.

Garrett, T.P., McKern, N.M., Lou, M., Elleman, T.C., Adams, T.E., Lovrecz, G.O., Kofler, M., Jorissen, R.N., Nice, E.C., Burgess, A.W., and Ward, C.W. (2003). The crystal structure of a truncated ErbB2 ectodomain reveals an active conformation, poised to interact with other ErbB receptors. Mol. Cell *11*, 495–505.

Graus-Porta, D., Beerli, R.R., Daly, J.M., and Hynes, N.E. (1997). ErbB-2, the preferred heterodimerization partner of all ErbB receptors, is a mediator of lateral signaling. EMBO J. *16*, 1647–1655.

Groenen, L.C., Walker, F., Burgess, A.W., and Treutlein, H.R. (1997). A model for the activation of the epidermal growth factor receptor kinase involvement of an asymmetric dimer? Biochemistry *36*, 3826–3836.

Hanks, S.K., and Hunter, T. (1995). Protein kinases 6. The eukaryotic protein kinase superfamily: kinase (catalytic) domain structure and classification. FASEB J. *9*, 576–596.

Holbro, T., Civenni, G., and Hynes, N.E. (2003). The ErbB receptors and their role in cancer progression. Exp. Cell Res. *284*, 99–110.

Hudziak, R.M., and Ullrich, A. (1991). Cell transformation potential of a HER2

transmembrane domain deletion mutant retained in the endoplasmic reticulum. J. Biol. Chem. *266*, 24109–24115.

Jorissen, R.N., Walker, F., Pouliot, N., Garrett, T.P., Ward, C.W., and Burgess, A.W. (2003). Epidermal growth factor receptor: mechanisms of activation and signalling. Exp. Cell Res. *284*, 31–53.

Kelley, R.F., O'Connell, M.P., Carter, P., Presta, L., Eigenbrot, C., Covarrubias, M., Snedecor, B., Bourell, J.H., and Vetterlein, D. (1992). Antigen binding thermodynamics and antiproliferative effects of chimeric and humanized anti-p185HER2 antibody Fab fragments. Biochemistry *31*, 5434–5441.

Livneh, E., Glazer, L., Segal, D., Schlessinger, J., and Shilo, B.Z. (1985). The Drosophila EGF receptor gene homolog: conservation of both hormone binding and kinase domains. Cell *40*, 599–607.

Mann, M., Sheng, H., Shao, J., Williams, C.S., Pisacane, P.I., Sliwkowski, M.X., and DuBois, R.N. (2001). Targeting cyclooxygenase 2 and HER-2/neu pathways inhibits colorectal carcinoma growth. Gastroenterology *120*, 1713–1719.

Mendoza, N., Phillips, G.L., Silva, J., Schwall, R., and Wickramasinghe, D. (2002). Inhibition of ligand-mediated HER2 activation in androgen-independent prostate cancer. Cancer Res. *62*, 5485–5488.

Molina, M.A., Codony-Servat, J., Albanell, J., Rojo, F., Arribas, J., and Baselga, J. (2001). Trastuzumab (herceptin), a humanized anti-Her2 receptor monoclonal antibody, inhibits basal and activated Her2 ectodomain cleavage in breast cancer cells. Cancer Res. *61*, 4744–4749.

Murali, R., Brennan, P.J., Kieber-Emmons, T., and Greene, M.I. (1996). Structural analysis of p185c-neu and epidermal growth factor receptor tyrosine kinases: oligomerization of kinase domains. Proc. Natl. Acad. Sci. USA *93*, 6252–6257.

Murshudov, G.N., Vagin, A.A., and Dodson, E.J. (1997). Refinement of Macromolecular Structures by the Maximum-Likelihood Method. Acta Crystallogr. D *53*, 240–255.

Navaza, J. (1994). AMoRe: an Automated Package for Molecular Replacement. Acta Crystallogr. A *50*, 157–163.

Ogiso, H., Ishitani, R., Nureki, O., Fukai, S., Yamanaka, M., Kim, J.H., Saito, K., Sakamoto, A., Inoue, M., Shirouzu, M., and Yokoyama, S. (2002). Crystal structure of the complex of human epidermal growth factor and receptor extracellular domains. Cell *110*, 775–787.

Olayioye, M.A., Neve, R.M., Lane, H.A., and Hynes, N.E. (2000). The ErbB signaling network: receptor heterodimerization in development and cancer. EMBO J. *19*, 3159–3167.

Paborsky, L.R., Fendly, B.M., Fisher, K.L., Lawn, R.M., Marks, B.J., McCray, G., Tate, K.M., Vehar, G.A., and Gorman, C.M. (1990). Mammalian cell transient expression of tissue factor for the production of antigen. Protein Eng. *3*, 547–553.

Paik, S., and Liu, E.T. (2000). HER2 as a predictor of therapeutic response in breast cancer. Breast Disease *11*, 91–102.

Ross, J.S., and Fletcher, J.A. (1998). The HER-2/neu oncogene in breast cancer: prognostic factor, predictive factor, and target for therapy. Stem Cells *16*, 413–428.

Schaefer, G., Akita, R.W., and Sliwkowski, M.X. (1999). A discrete three-amino acid segment (LVI) at the C-terminal end of kinase-impaired ErbB3 is required for transactivation of ErbB2. J. Biol. Chem. *274*, 859–866.

Schlessinger, J. (2000). Cell signaling by receptor tyrosine kinases. Cell *103*, 211–225.

Slamon, D.J., Clark, G.M., Wong, S.G., Levin, W.J., Ullrich, A., and McGuire, W.L. (1987). Human breast cancer: correlation of relapse and survival with amplification of the HER-2/neu oncogene. Science *235*, 177–182.

Slamon, D.J., Leyland-Jones, B., Shak, S., Fuchs, H., Paton, V., Bajamonde, A., Fleming, T., Eiermann, W., Wolter, J., Pegram, M., et al. (2001). Use of chemotherapy plus a monoclonal antibody against HER2 for metastatic breast cancer that overexpresses HER2. N. Engl. J. Med. *344*, 783–792.

Stamos, J., Sliwkowski, M.X., and Eigenbrot, C. (2002). Structure of the epidermal growth factor receptor kinase domain alone and in complex with a 4-anilinoquinazoline inhibitor. J. Biol. Chem. *277*, 46265–46272.

Stein, R.A., and Staros, J.V. (2000). Evolutionary analysis of the ErbB receptor and ligand families. J. Mol. Evol. *50*, 397–412.

Vajdos, F.F., Adams, C.W., Breece, T.N., Presta, L.G., de Vos, A.M., and Sidhu, S.S. (2002). Comprehensive functional maps of the antigen-binding site of an anti-ErbB2 antibody obtained with shotgun scanning mutagenesis. J. Mol. Biol. *320*, 415–428.

Vogel, C.L., Cobleigh, M.A., Tripathy, D., Gutheil, J.C., Harris, L.N., Fehrenbacher, L., Slamon, D.J., Murphy, M., Novotny, W.F., Burchmore, M., et al. (2002). Efficacy and safety of trastuzumab as a single agent in first-line treatment of HER2-overexpressing metastatic breast cancer. J. Clin. Oncol. *20*, 719–726.

Wadsworth, S.C., Vincent, W.S., 3rd, and Bilodeau-Wentworth, D. (1985). A Drosophila genomic sequence with homology to human epidermal growth factor receptor. Nature *314*, 178–180.

Ward, C.W., and Garrett, T.P. (2001). The relationship between the L1 and L2 domains of the insulin and epidermal growth factor receptors and leucine-rich repeat modules. BMC Bioinformatics *2*, 4.

Werther, W.A., Gonzalez, T.N., O'Connor, S.J., McCabe, S., Chan, B., Hotaling, T., Champe, M., Fox, J.A., Jardieu, P.M., Berman, P.W., and Presta, L.G. (1996). Humanization of an anti-lymphocyte function-associated antigen (LFA)-1 monoclonal antibody and reengineering of the humanized antibody for binding to rhesus LFA-1. J. Immunol. *157*, 4986–4995.

Yarden, Y., and Sliwkowski, M.X. (2001). Untangling the ErbB signalling network. Nat. Rev. Mol. Cell Biol. *2*, 127–137.

Accession numbers

The ErbB2-pertuzumab complex structure has been deposited with the RCSB Protein Data Bank (ID code 1S78).